

# Structural and Single Crystal EPR Studies of the Complex Copper L-Glutamine: A Weakly Exchange-Coupled System with *syn-anti* Carboxylate Bridges

José M. Schweigkardt,<sup>[a]</sup> Alberto C. Rizzi,<sup>[a]</sup> Oscar E. Piro,<sup>[b]</sup> Eduardo E. Castellano,<sup>[c]</sup> Ricardo Costa de Santana,<sup>[d]</sup> Rafael Calvo,<sup>[a,e]</sup> and Carlos D. Brondino\*<sup>[a]</sup>

**Keywords:** EPR spectroscopy / Carboxylate ligands / Through bond interactions / Copper / Magnetic Properties / Layered compounds

We report the molecular structure and a single crystal EPR study at 9.8 and 33.9 GHz of a new copper(II) compound with the amino acid L-Glutamine,  $\text{Cu}[\text{NH}_2\text{CO}_2\text{CH}(\text{CH}_2)_2\text{CONH}_2]_2$ . The  $\text{Cu}^{\text{II}}$  ion is in an elongated octahedral environment equatorially *trans*-coordinated by two glutamine molecules acting as bidentate ligands through the nitrogen atom and one oxygen atom of each amino acid group, and axially by two carboxylate oxygen atoms of two neighboring glutamine molecules. Copper ions are arranged in layers connected by *syn-anti* carboxylate bridges that provide equatorial and apical ligands to the copper ions. Neighboring layers are connected by long chemical paths, which include two amino acid side chains connected by H bonds. Single crystal EPR spectra show a single exchange-collapsed resonance at both microwave frequencies for any magnetic field orientation. The evaluation of the molecular *g*-tensor from the angu-

lar variation of the EPR line position yielded  $g_{\perp} = 2.051$  and  $g_{\parallel} = 2.248$ , which indicates a  $d_{x^2-y^2}$  ground orbital for the  $\text{Cu}$  ions. The angular variation of the EPR line width displays a contribution that is typical of a 2-D magnetic system, and another contribution depending on the microwave frequency, which is attributed to the incomplete collapse of the resonances corresponding to magnetically nonequivalent copper ions. A quantitative analysis of the line width data allowed us to estimate a mean exchange coupling constant  $|J/k| = 0.42(2)$  K, which is assigned to the *syn-anti* carboxylate chemical path that connects neighboring copper ions within a layer. The results are discussed and compared with those observed in similar systems.

(© Wiley-VCH Verlag GmbH, 69451 Weinheim, Germany, 2002)

## Introduction

Copper complexes with amino acids are appropriate compounds for the study of magnetic properties of weakly exchange-coupled systems. They are also of biological interest as amino acids provide ligands to the metal ions in metalloproteins.<sup>[1]</sup> Additional biological interest arises because chemical paths for superexchange interactions, such as carboxylate bridges, saturated and nonsaturated sigma bonds, hydrogen bonds, stacking of aromatic rings, or

mixed paths integrated by fragments of the previous ones, have been identified as possible pathways for electron transfer in several biological systems.<sup>[2]</sup> These paths are responsible for the transmission of weak exchange interactions ( $0.0005 \text{ K} \leq |J/k| \leq 2 \text{ K}$ ) that have been related to the matrix element for electron transfer between redox centers in metalloproteins.<sup>[3]</sup> Small exchange interactions are difficult to evaluate by standard magnetic susceptibility measurements, but they can be accurately and selectively measured employing EPR spectroscopy.<sup>[4–6]</sup>

Most solid copper compounds with  $\alpha$ -amino acids have the  $\text{Cu}^{\text{II}}$  ions coordinated to the nitrogen and one of the carboxylate oxygen atoms of the amino acid group of two amino acid molecules, while the remaining carboxylate oxygen atoms are bonded to copper ions of neighboring molecules. This gives rise to copper ion networks having 1-, 2-, or 3-D structures, connected by carboxylate bridges of the *syn-anti* type that provide equatorial and apical ligands to the copper ions.<sup>[7–12]</sup> A different situation occurs in the copper complexes with aspartic acid,<sup>[13,14]</sup> glutamic acid,<sup>[15,16]</sup> and asparagine.<sup>[17]</sup> In these compounds, the copper ions are coordinated to one amino acid molecule as

<sup>[a]</sup> Departamento de Física, Facultad de Bioquímica y Ciencias Biológicas, Universidad Nacional del Litoral C.C. 242, 3000 Santa Fe, Argentina Fax: (internat.) + 54–342/4575221 E-mail: brondino@dfbioq.unl.edu.ar

<sup>[b]</sup> Departamento de Física, Facultad de Ciencias Exactas, Universidad Nacional de La Plata and Instituto IFLP (CONICET) C.C. 67, 1900 La Plata, Argentina

<sup>[c]</sup> Instituto de Física de São Carlos, Universidade de São Paulo C.P. 369, 13560 São Carlos (SP), Brazil

<sup>[d]</sup> Instituto de Física, Universidade Federal de Goiás, Campus Samambaia, C.P. 131, 74001–970, Goiânia-GO, Brazil

<sup>[e]</sup> INTEC (CONICET–UNL) Güemes 3450, 3000 Santa Fe, Argentina

in the compounds described above, and, in addition, are coordinated to the side chain carboxylate group of the other amino acid molecule in the case of aspartic and glutamic acids, and by the side chain amide in the case of asparagine. This coordination gives rise to polymeric chains, where the sigma skeleton of the amino acid molecule connects two neighboring copper ions.

We report herein the crystal and molecular structure and a single-crystal EPR study of the copper complex with the amino acid L-glutamine. According to the information given above, this compound was expected to exhibit a polymeric structure. However, our results indicate that this complex has a molecular structure and a magnetic behaviour different from that observed in polymeric compounds.

## Results and Discussion

### Molecular Structure

X-ray structural characterizations of the title compound reveal that it crystallizes in the monoclinic space group  $C2$ . The copper ion has an elongated octahedral coordination, trans coordinated by two glutamine molecules with a nearly square planar equatorial  $N_2O_2$  ligand group. Figure 1 is an ORTEP<sup>[18]</sup> drawing of the complex showing the coordination around the  $Cu^{II}$  ion, hereafter called  $Cu(gln)_2$ . Selected bond lengths and angles are given in Table 1. The axial ligands are the carboxylate oxygen atoms O22 and O12, each belonging to one of two symmetry related neighboring glutamine molecules.

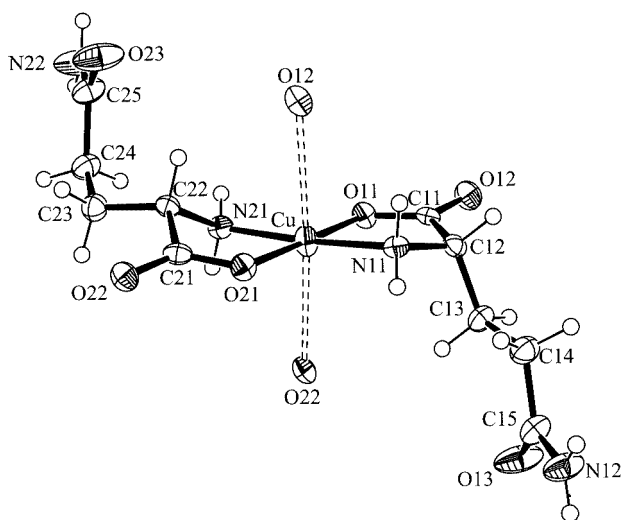


Figure 1. Drawing of the  $Cu(gln)_2$  molecule showing the coordination around  $Cu^{II}$ , the labeling scheme of the non-H atoms and their displacement ellipsoids at 50% probability level; full lines indicate copper-ligand bonds

The four symmetry related copper ions in the unit cell of  $Cu(gln)_2$  lie in two layers parallel to the  $cb$  plane 14.1 Å apart. One of them, shown in Figure 2, contains the copper atoms in the general positions  $(x, y, z)$  and  $(-x + 1/2, y + 1/2, -z)$  (positions I and IV, respectively, of the crystallo-

Table 1. Selected bond lengths (Å) and angles (deg) around copper(II) for  $Cu(gln)_2$ ; symmetry code: (i)  $3/2-x, y-1/2, 2-z$ ; (ii)  $3/2-x, y+1/2, 1-z$ .

Bond lengths		Bond angles	
Cu–O(11)	1.941(2)	O(21)–Cu–O(11)	179.10(7)
Cu–O(21)	1.951(2)	O(11)–Cu–N(11)	84.39(7)
Cu–N(11)	1.985(2)	O(11)–Cu–N(21)	95.62(8)
Cu–N(21)	1.984(2)	O(21)–Cu–N(21)	84.11(7)
Cu–O(12 <sup>i</sup> )	2.848(3)	N(11)–Cu–N(21)	175.44(9)
Cu–O(22 <sup>ii</sup> )	2.778(3)	O(12 <sup>i</sup> )–Cu–O(22 <sup>ii</sup> )	176.11(13)

graphic space group  $C2$ ). The other one contains the copper atoms in positions  $(-x, y, -z)$  and  $(x + 1/2, y + 1/2, z)$  (positions II and III, respectively).<sup>[19]</sup>

Two different types of chemical paths connect copper ions within each layer.  $Cu^I$  and  $Cu^{IV}$  are connected by two similar carboxylate bridges of the *syn-anti* type ( $-Cu-O_{ap}-C-O_{eq}-Cu-$ ), which gives rise to a 2-D network of copper ions (see Figure 2). The same situation occurs for  $Cu^{II}$  and  $Cu^{III}$  in the other layer (not shown). A similar equatorial-apical copper interaction in the layered compounds has been observed in the copper complexes with the amino acids phenylalanine,<sup>[7]</sup> methionine,<sup>[8]</sup> leucine,<sup>[9]</sup> alanine,<sup>[10,11]</sup> and  $\alpha$ -aminobutyric acid.<sup>[12]</sup> The second path is provided by double hydrogen bonds  $N-H\cdots O$  that connect the copper ions with identical spatial orientation (Figure 2). This connection, which involves equatorial ligands to the copper ions, gives rise to infinite polymeric chains along the  $b$  crystal axis. Copper ions having the same spatial orientation, but in neighboring layers, are connected by chemical paths that involve the skeleton of two amino acid molecules and double  $N-H\cdots O$  hydrogen bonds (see Figure 3).

### Crystal and Molecular $g$ -Factor

The room temperature EPR spectra of  $Cu(gln)_2$  display a single Lorentzian-shaped resonance line for any magnetic field orientation at the microwave frequencies of 9.8 and 33.9 GHz. Figure 4 shows the angular variation of the squared  $g$ -factor [ $g^2(\theta, \phi)$ ] observed at 9.8 GHz. A similar result is obtained at 33.9 GHz (data not shown). Since  $Cu^I$  and  $Cu^{III}$  sites [as well as  $Cu^{II}$  and  $Cu^{IV}$ ] are related by a  $[1/2, 1/2, 0]$  translation, they have identical spatial orientation and consequently give rise to identical EPR spectra for any magnetic field orientation. Within each layer  $Cu^I$  and  $Cu^{IV}$  sites [as well as  $Cu^{II}$  and  $Cu^{III}$ ] are related by a  $C_{2b}$  rotation, and consequently the angular variation of their EPR spectra will also be related by the same symmetry operation. Therefore, two-symmetry related EPR spectra associated with copper ion pairs I–III and II–IV are expected for any magnetic field orientation except in the  $ca$  plane and along the  $b$  crystal axis, in which the four copper ions are magnetically equivalent. These resonance lines should be split by hyperfine interactions with the copper nuclear spin ( $I = 3/2$ ) and the nitrogen ligands ( $I = 1$ ). The fact that a single Lorentzian-shaped resonance line is observed for the

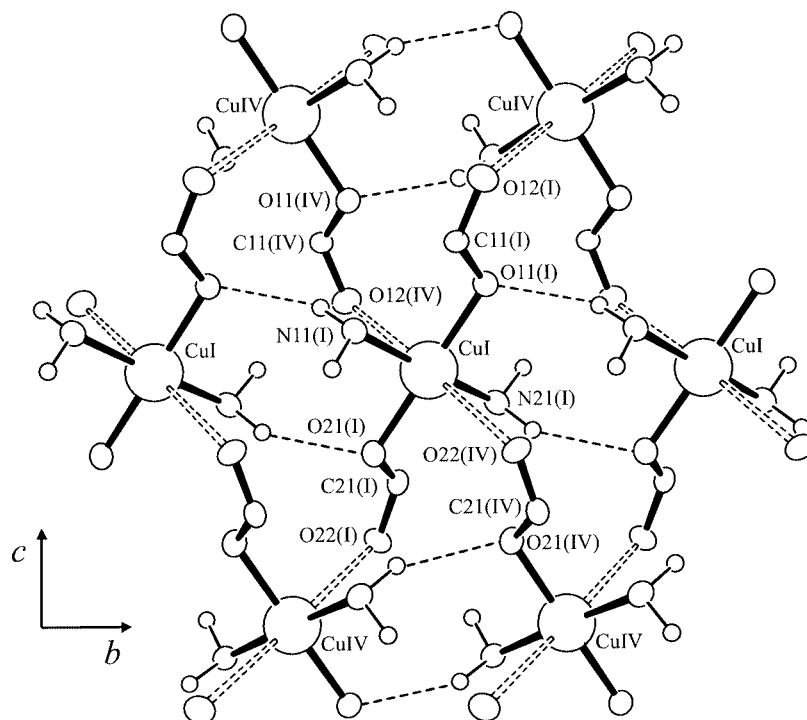


Figure 2. Orthogonal projection of  $\text{Cu}(\text{gln})_2$  along  $a^* = b \times c$  crystal axis showing a copper atom and its six nearest copper neighbors within a layer; only the layer containing copper ions at symmetry positions I and IV is shown

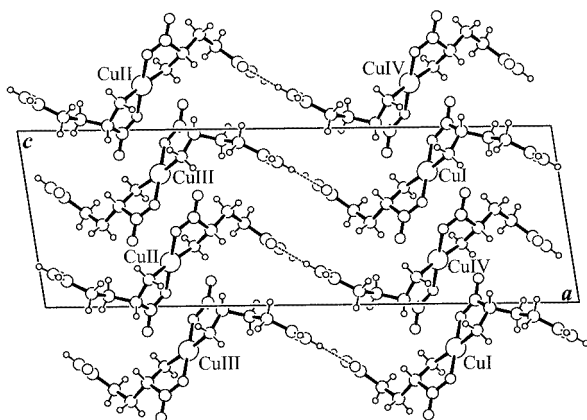


Figure 3. Orthogonal projection of  $\text{Cu}(\text{gln})_2$  along the  $b$  crystal axis showing the copper atom layers and the chemical paths connecting them

measured crystal planes, even at 33.9 GHz, indicates that the exchange interaction between the  $\text{Cu}^{\text{II}}$  ions is large enough to collapse both the expected hyperfine splitting and the resonance lines due to magnetically nonequivalent  $\text{Cu}^{\text{II}}$  ions.

For a magnetic system showing a single exchange-collapsed resonance line, the position of the observed resonance lines is described by the Zeeman Hamiltonian in Equation (1) where  $\mu_B$  is the Bohr magneton,  $\mathbf{S}$  is the effective spin operator ( $S = 1/2$ ),  $\mathbf{g}$  is the crystal  $\mathbf{g}$ -tensor defined as the average of the molecular  $\mathbf{g}_i$ -tensors ( $i = \text{I}, \dots, \text{IV}$ ), and  $\mathbf{B}$  is the applied magnetic field.

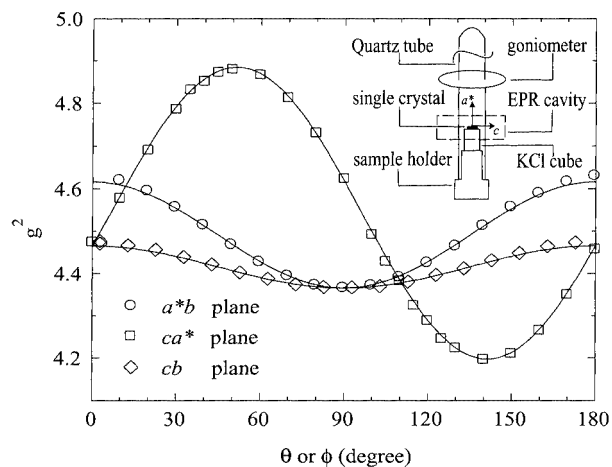


Figure 4. Angular variation of the squared  $g$ -factor measured at 298 K and 9.8 GHz in three orthogonal crystalline planes of  $\text{Cu}(\text{gln})_2$ ; the solid lines were obtained by fitting a symmetric  $g^2$  second-order tensor to the data; the parameters of the fit are included in Table 2; the inset schematizes the orientation of the sample for the EPR experiment

$$H = \mu_B \mathbf{S} \cdot \mathbf{g} \cdot \mathbf{B} \quad (1)$$

The components of the crystal  $\mathbf{g}$ -tensor defined in Equation (1) were obtained by least-squares fitting the function  $g^2(\theta, \phi) = \mathbf{h} \cdot \mathbf{g}^2 \cdot \mathbf{h}$  to the experimental data, where  $\mathbf{h} = \mathbf{B}/|\mathbf{B}| = (\sin\theta \cos\phi, \sin\theta \sin\phi, \cos\theta)$  is the direction of the applied magnetic field  $\mathbf{B}$ . The components of  $\mathbf{g}^2$  at both microwave frequencies, its eigenvalues and eigenvectors, are

given in Table 2. They were employed to calculate the solid lines shown in Figure 4.

Table 2. Values of the components of the  $g^2$  tensor obtained by least-squares analyses of the data at both microwave frequencies.  $(g^2)_1$ ,  $(g^2)_2$  and  $(g^2)_3$  and  $\mathbf{a}_1$ ,  $\mathbf{a}_2$  and  $\mathbf{a}_3$  are the eigenvalues and eigenvectors of the  $g^2$  tensor in the  $xyz = a^*bc$  coordinates system ( $a^* = b \times c$ ); the values of  $g_{\perp}$  and  $g_{\parallel}$ , the polar and azimuthal angles  $\theta_m$  and  $\phi_m$ , of the normal to the square of ligands to copper ion in site I, and the angle  $2\alpha$  between the normals to copper ions in sites I and IV (identical to those of sites II and III) were calculated like in ref.<sup>[20]</sup>

9.8 GHz	33.9 GHz
$(g^2)_{xx} = 4.616(1)$	$(g^2)_{xx} = 4.6036(5)$
$(g^2)_{yy} = 4.366(1)$	$(g^2)_{yy} = 4.3918(5)$
$(g^2)_{zz} = 4.466(1)$	$(g^2)_{zz} = 4.4865(5)$
$(g^2)_{zx} = 0.33(5)$	$(g^2)_{zx} = 0.3255(5)$
$(g^2)_{xy} = (g^2)_{zy} = 0$	$(g^2)_{xy} = (g^2)_{zy} = 0$
$(g^2)_1 = 4.197(1)$	$(g^2)_1 = 4.2143(5)$
$(g^2)_2 = 4.884(1)$	$(g^2)_2 = 4.8758(5)$
$(g^2)_3 = 4.366(1)$	$(g^2)_3 = 4.3918(5)$
$\mathbf{a}_1 = [0.625(1), 0, 0.7808(1)]$	$\mathbf{a}_1 = [0.6415(3), 0, 0.7672(3)]$
$\mathbf{a}_2 = [0.7808(1), 0, -0.625(1)]$	$\mathbf{a}_2 = [0.7672(3), 0, -0.6415(3)]$
$\mathbf{a}_3 = [0, 1, 0]$	$\mathbf{a}_3 = [0, 1, 0]$
$g_{\perp} = 2.049$	$g_{\perp} = 2.053$
$g_{\parallel} = 2.248$	$g_{\parallel} = 2.248$
$2\alpha = 127.3^\circ$	$2\alpha = 125.2^\circ$
$\theta_m = 124.1$	$\theta_m = 124.7$
$\phi_m = 32.3$	$\phi_m = 34.0$

The components and principal directions of the copper molecular  $g$ -tensor shown in Table 2 were evaluated following the procedure described elsewhere assuming axial symmetry.<sup>[20]</sup>  $\theta_m$  and  $\phi_m$  are, respectively, the polar and azimuthal angles of the symmetry axis of the  $\text{Cu}^{\text{I}}$  site [identical to  $\text{Cu}^{\text{III}}$  site] referred as to the  $a^*bc$  crystal system, and  $2\alpha$  is the angle between the normals to the  $\text{Cu}^{\text{I}}$  and  $\text{Cu}^{\text{IV}}$  sites [identical to  $\text{Cu}^{\text{II}}-\text{Cu}^{\text{III}}$ ]. The values for  $\theta_m$ ,  $\phi_m$  and  $2\alpha$  are in a good agreement with the crystallographic ones ( $\theta_c = 120.4^\circ$ ,  $\phi_c = 29.0^\circ$ , and  $2\alpha_c = 130.4^\circ$ ), supporting the assumption of axial symmetry for this copper complex. The result obtained for the molecular  $g$ -tensor (Table 2) indicates a  $d_{x^2-y^2}$  ground state orbital situated in the equatorial ligand plane of the  $\text{Cu}^{\text{II}}$  ion.<sup>[21]</sup>

### EPR Line Width and Superexchange Paths

Figure 5 shows the angular variation of the peak-to-peak line width [ $\Delta B_{\text{pp}}(\theta, \phi)$ ] at 9.8 and 33.3 GHz. To analyze the variation of the line width with the magnetic field orientation, the data shown in Figure 5 were least-squares fitted with the function presented in Equation (2), where  $\theta_n$  is the angle between the applied external magnetic field and the normal to the layers ( $\cos\theta_n = \sin\theta \cos\phi$ ). The  $a_i$  coefficients, given in Table 3, were used to obtain the solid lines shown in Figure 5.

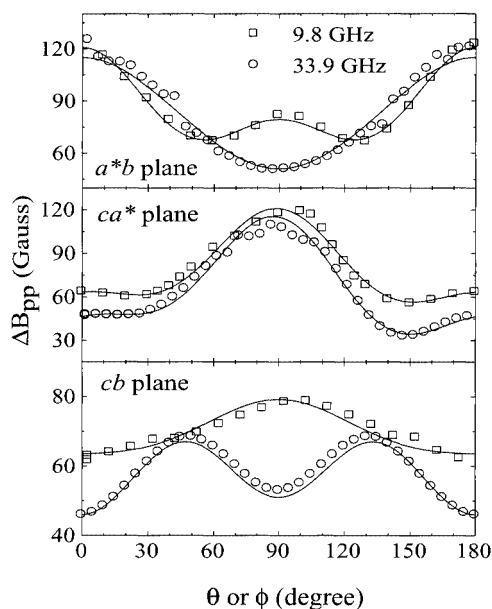


Figure 5. Angular variation of the peak-to-peak line width measured at 9.8 GHz and 33.9 GHz and 298 K in three orthogonal crystalline planes of  $\text{Cu}(\text{gln})_2$ ; the solid lines were obtained by fitting the data with Equation (2); the parameters of the fit are included in Table 3

Table 3. Values of the coefficients  $a_i$  (in Gauss) obtained at each microwave frequency by least-squares analyses of the line width data to Equation (2)

	9.8 GHz	33.9 GHz
$a_1$	75(1)	63(1)
$a_2$	66(1)	38(1)
$a_3$	52(1)	34(1)
$a_4$	7(1)	17(2)
$a_5$	11.7(1)	13.2(5)
$a_6$	n.d. <sup>[a]</sup>	1801(81)

[a] n.d. not detectable

$$\Delta B_{\text{pp}}(\theta, \phi) = a_1 \sin^2\theta \cos^2\phi + a_2 \sin^2\theta \sin^2\phi + a_3 \cos^2\theta + a_4 \sin\theta \cos\theta \cos\phi + a_5 (1 - 3 \cos^2\theta_n)^2 + a_6 [g_{\text{I}}(\theta, \phi) - g_{\text{IV}}(\theta, \phi)]^2 \quad (2)$$

Several mechanisms, such as dipolar interactions and incomplete collapse of the hyperfine splitting and/or the resonances corresponding to nonequivalent copper ions, contribute to the EPR line width in copper amino acid complexes.<sup>[22–25]</sup> The terms  $a_{1-4}$  in Equation (2) consider the contributions to the EPR line width of interactions having a second order angular variation, like the crystal  $g$ -tensor, such as the incomplete collapse of the hyperfine structure, as well as other smaller interactions (e.g. anisotropic and antisymmetric exchange).<sup>[4]</sup> They are not important in our study, and therefore will not be analyzed further.

The term  $a_5$  describes the dipolar contribution for a 2-D magnetic system.<sup>[26]</sup> The typical angular variation originat-

ing from this interaction can be visualized at the X-band in Figure 5. At the Q-band, the contribution of the dipolar interaction in both  $a^*b$  and  $cb$  planes is masked by the contribution described by the term  $a_6$ , which is negligible at the X-band but not at the Q-band (see below).

The term  $a_6$  in Equation (2) takes into account the contribution to the line width arising from the presence of two magnetically nonequivalent copper sites in the crystal lattice of  $\text{Cu}(\text{gln})_2$ . As discussed elsewhere,<sup>[27,28]</sup> this interaction depends on both the microwave frequency and the number of neighboring nonequivalent  $\text{Cu}^{\text{II}}$  ions connected by the bridge. Its contribution can be identified at the Q-band in the  $cb$  and, though less noticeable,  $a^*b$  crystal planes (see Figure 5 and Table 3). On the contrary, in the  $ca^*$  crystal plane, where the four copper ions are magnetically equivalent, the line width does not show significant differences at both frequencies, except for a small constant shift. This shift is attributed to nonsecular terms of the Zeeman interaction that only make a contribution at the X-band.<sup>[29]</sup>

For a system having two magnetically nonequivalent copper ions per unit cell, the coefficient  $a_6$  in Equation (2) is given by Equation (3),<sup>[28,30]</sup> where  $g = 1/3 \text{tr}(\mathbf{g})$  is the isotropic  $g$ -factor,  $\omega_0$  is the Larmor frequency, and  $\omega_e$  is the exchange frequency.

$$a_6 = (2/3\pi)^{1/2} \omega_0^2 \hbar/4 g^3 \omega_e \mu_B \quad (3)$$

Using Equation (3) and the  $a_6$  value obtained from the fitting (Table 3 and Figure 5) we calculated  $\omega_e = 1.089 \times 10^{11} \text{ s}^{-1}$ , which is related to the exchange parameters through Equation (4)<sup>[28]</sup> where  $J_i$ 's are the exchange parameters associated with the chemical paths connecting magnetically nonequivalent copper ion pairs and  $z_i$  is the number of the nearest neighboring copper ions connected by the  $i$ th chemical path.

$$\hbar \omega_e = (\sum_i z_i J_i^2)^{1/2} \quad (4)$$

As shown in Figures 2 and 3, each copper ion is connected to only four nonequivalent neighboring copper ions through two similar *syn-anti* carboxylate bridges. Further, since line-width data indicate a 2-D magnetic behaviour, it is reasonable to assume  $J_1 \approx J_2$ , where  $J_1$  and  $J_2$  are the exchange parameters associated with each carboxylate bridge. Then, from Equation (4) we obtain a mean exchange parameter  $|J|/k = 0.42(2) \text{ K}$  for the intralayer bridge connecting magnetically nonequivalent copper ions (Figure 2).<sup>[31]</sup> This value is supported by the lowest limit  $|J|/k \geq 0.13 \text{ K}$  estimated from the collapse condition  $J \geq \Delta g \mu_B B$  at Q-band. The model employed to analyze the EPR data does not allow for the measurement of exchange couplings between magnetically equivalent copper ions associated with intra- or interlayer bridges (Figures 2 and 3). However, the observed 2-D spin dynamic indicates that the interlayer exchange couplings are negligible (Figure 3). Thermodynamic measurements at very low temperatures ( $< 1 \text{ K}$ ) performed on the copper compounds with the amino acids

L-alanine<sup>[32,33]</sup> and  $\alpha$ -aminobutyric acid<sup>[34]</sup> indicate that *syn-anti* carboxylate bridges involving equatorial and apical ligands to the copper ions transmit antiferromagnetic interactions. Therefore, a similar magnetic behaviour is expected for all copper amino acid compounds that show this characteristic.

Levstein and Calvo observed that the magnitude of  $J$  decreases linearly with an increase in the  $\text{Cu}-\text{O}_{\text{ap}}$  bond length for three  $\text{Cu}^{\text{II}}$  amino acid complexes.<sup>[35]</sup> According to their results, the  $J$  value for  $\text{Cu}(\text{gln})_2$  should be smaller than  $0.1 \text{ K}$ . A similar discrepancy was obtained for the copper complexes with L-alanine<sup>[32]</sup> and L- $\alpha$ -aminobutyric acid.<sup>[12]</sup> Thus, the length of the  $\text{Cu}-\text{O}_{\text{ap}}$  bond is not the only factor that determines the magnitude of the magnetic interactions, but other structural factors should also be considered. Table 4 shows the  $J$  values, the  $\text{Cu}-\text{O}_{\text{ap}}$  distances and the dihedral angles between the plane of the carboxylate bridge and the planes (eq and eq') of the equatorial ligands of the two magnetically nonequivalent  $\text{Cu}^{\text{II}}$  ions connected by the bridge for six layered  $\text{Cu}^{\text{II}}$  L-amino acid complexes. As seen in Table 4, the compounds studied in ref.<sup>[35]</sup> have similar dihedral angles, deviating by about two degrees from the mean value. Meanwhile, the compounds that do not follow the proposed dependence of the magnitude of  $J$  with the  $\text{Cu}-\text{O}_{\text{ap}}$  length have smaller dihedral angles when the longer  $\text{Cu}-\text{O}_{\text{ap}}$  bond is taken into account. For the shorter  $\text{Cu}-\text{O}_{\text{ap}}$  bond, there is a dual behaviour: on the one hand no significant changes are observed for the higher angles ( $< \text{eq}-\text{OCO}$  in Table 4); on the other hand, a slight increase of the angle value is observed for the lower angles ( $< \text{eq}'-\text{OCO}$  in Table 4). Consequently, the results in Table 4 suggest that the values of the angles between the magnetic orbitals of the  $\text{Cu}^{\text{II}}$  ion and the OCO plane, play a key role regarding the  $J$  value. They indicate that the higher the planarity of the  $\text{Cu}-\text{OCO}-\text{Cu}$  bridge, the larger the magnitude of the exchange interaction. This is in line with previous observations for some copper dimers, which yielded the same conclusion.<sup>[36]</sup>

Table 4.  $J$ -values, copper-apical ligand bond lengths, and angles between the carboxylate group bridging equatorial ligand planes of two nearest magnetically nonequivalent  $\text{Cu}^{\text{II}}$  ions (eq and eq') in six layered  $\text{Cu}^{\text{II}}$ -L-amino acid complexes

Compound	$ J /k$ [K]	$d_{\text{Cu}-\text{O}_{\text{ap}}}$ [Å]	$\angle \text{eq}-\text{OCO}$ [°]	$\angle \text{eq}'-\text{OCO}$ [°]	Ref
$\text{Cu}(\text{met})_2$	0.10(1)	2.675	75.2	17.7	[8,35]
		2.751	67.8	10.8	
$\text{Cu}(\text{leu})_2$	0.23(1)	2.628	79.2	18.1	[9,35]
		2.749	72.2	12.0	
$\text{Cu}(\text{phe})_2$	0.38(2)	2.578	77.4	16.4	[7,35]
		2.690	71.0	10.9	
$\text{Cu}(\text{ala})_2$	0.33(1)	2.698	75.9	21.8	[10,11,32]
		2.904	58.5	6.6	
$\text{Cu}(\text{but})_2$	0.36(3)	2.676	73.1	16.3	[12]
		2.783	64.9	9.1	
$\text{Cu}(\text{gln})_2$	0.42(2)	2.778	72.4	19.7	This work
		2.848	59.9	7.7	

## Conclusion

This work demonstrates that  $\text{Cu}(\text{gln})_2$  belongs to the family of copper amino acid complexes in which the amino acid R group is not involved in the  $\text{Cu}^{\text{II}}$  coordination resulting in a layered structure of copper ions connected by equatorial-apical *syn-anti* carboxylate bridges.  $\text{Cu}^{\text{II}}$  complexes of amino acids are among the few examples of equatorial-apical *syn-anti* carboxylate-bridged compounds magnetically characterized so far.<sup>[37]</sup> In this work we show that the magnitude of the exchange interaction depends on both the  $\text{Cu}-\text{O}_{\text{ap}}$  distance and the angles between the equatorial ligand plane and the bridging ligand plane. The larger the co-planarity between the  $\text{Cu}^{\text{II}}$  equatorial ligand plane and the OCO plane, the larger the  $J$  value.

## Experimental Section

**Sample Preparation:** All commercially available chemicals were reagent grade and used without further purification. Single crystals of  $\text{Cu}(\text{gln})_2$ ,  $\text{Cu}[\text{NH}_2\text{CO}_2\text{CH}(\text{CH}_2)_2\text{CONH}_2]_2$ , were obtained by dissolving L-glutamine (730.5 mg, 5 mmol) and basic copper carbonate (276.4 mg, 2.5 mmol) in ion-exchanged water (40 mL). This solution was stirred for a few minutes until a light-blue colour developed, and the solid was filtered out, using a 0.22  $\mu\text{m}$  Millipore filter. The pH of the resulting solution was adjusted to 9 and left to evaporate at room temperature. Thin blue plates were obtained after one week. The crystals are elongated along the  $b$  direction and show well defined  $bc$  lateral faces.

**X-ray Structural Determination. Data Collection, Solution, and Refinement of the Structure.** X-ray data were collected at 120 and 293 K on an Enraf–Nonius KappaCCD diffractometer with  $\text{Mo-K}\alpha$  ( $\lambda = 0.71073 \text{ \AA}$ ) graphite monochromated radiation. Diffraction data were reduced and corrected using the DENZO and SCALEPACK Programs.<sup>[38]</sup> Structures were solved by direct methods with the help of the SHELXS-97 program<sup>[39]</sup> and refined on reflection intensities ( $F^2$ ) using the SHELXL-97 program.<sup>[40]</sup>

Table 5. Summary of the crystal data, intensity collection, and structure refinement parameters for  $\text{Cu}(\text{gln})_2$ .

Formula	$\text{C}_{10}\text{H}_{18}\text{CuN}_4\text{O}_6$
Crystal size (mm)	$0.08 \times 0.06 \times 0.02$
Molecular mass	353.82
Space group	$C2$
Crystal system	monoclinic
$a$ (Å)	28.0610(5)
$b$ (Å)	5.0756(1)
$c$ (Å)	9.3719(2)
$\beta$ (deg)	99.5139(8)
$Z$	4
$d_{\text{calcd.}}$ ( $\text{g}/\text{cm}^3$ )	1.785
Absorption coefficient ( $\text{mm}^{-1}$ )	1.695
$\theta$ range for data collection (deg)	2.20 to 25.77
Reflections collected/unique	12752/2288 [ $R(\text{int}) = 0.092$ ]
Data/restraints/parameters	2288/5/206
Goodness-of-fit on $F^2$	1.069
Final $R$ indices [ $I > 2\sigma(I)$ ] <sup>[a]</sup>	$R1 = 0.0214$ , $wR2 = 0.0559$

<sup>[a]</sup>  $R$  indices defined as:  $R1 = \sum ||F_o| - |F_c|| / \sum |F_o|$ ,  $wR2 = [\sum w(F_o^2 - F_c^2)^2 / \sum w(F_o^2)^2]^{1/2}$ .

Crystal data, structure determination methods and refinement results at 120 K are summarized in Table 5. All H atoms were located among the first 18 peaks of a difference Fourier map. As expected, the terminal amine H atoms were found close to the OCN plane. These hydrogen atoms were therefore positioned stereochemically on the corresponding planes and refined with the riding model. The hydrogen atoms of the amine group coordinated to the copper(II) ion were refined isotropically with N–H bond lengths restrained to a target value of 0.89(1) Å. The remaining glutamine H atoms were also positioned on a stereochemical basis and refined with the riding model. The room temperature solid is isomorphous to that of the low temperature one.

CCDC-179785 contains the supplementary crystallographic data for this paper. These data can be obtained free of charge at [www.ccdc.cam.ac.uk/conts/retrieving.html](http://www.ccdc.cam.ac.uk/conts/retrieving.html) [or from the Cambridge Crystallographic Data Centre, 12, Union Road, Cambridge CB2 1EZ, UK; Fax: (internat.) +44-1223/336-033; E-mail: [deposit@ccdc.cam.ac.uk](mailto:deposit@ccdc.cam.ac.uk)].

**EPR Measurements:** EPR spectra at 9.8 GHz (X-band) and 33.9 GHz (Q-band) were acquired on Bruker ER-200 and Bruker ESP300 spectrometers, respectively, using a Bruker rectangular cavity ER4102ST (X-band) and a cylindrical cavity ER5101Q (Q-band). The field modulation was 100 kHz in both cases. All the experiments were carried out at room temperature.

The samples were oriented by gluing the single crystal  $bc$  face to a cleaved KCl cubic holder, which defines a set of  $x, y, z$  orthogonal axes with the  $x$  axis along the  $a^* = b \times c$  direction, and the  $y$  and  $z$  directions along the  $b$  and  $c$  crystal axes, respectively. For the X-band measurements, the sample holder was positioned on the horizontal plane at the top of a pedestal, which was introduced into a 4 mm OD Quartz tube (see inset on Figure 4). For the Q-band measurements, the samples were mounted only on the pedestal. Both devices were introduced into the cavity, and the EPR spectra were taken with the magnetic field along several directions of the crystal planes  $a^*b$ ,  $ca^*$  and  $cb$  of the sample. Positions and peak-to-peak line widths ( $\Delta B_{pp}$ ) of the resonance lines were obtained by least-squares fitting of the spectra to a Lorentzian derivative line.

## Acknowledgments

This work was supported by the Universidad Nacional del Litoral (CAI+D 291) (Argentina), the Consejo Nacional de Investigaciones Científicas y Técnicas (CONICET) (Argentina), Fundación Antorchas (Argentina), the Conselho Nacional de Pesquisas (CNPq) (Brazil), and the Fundação de Amparo a Pesquisa do Estado de São Paulo (FAPESP) (Brazil). We thank Dr. Fernando Pelegrini (UFG, Brazil) in whose lab we performed the Q-band EPR measurements.

- [1] S. J. Lippard, J. M. Berg, *Principles of Bioinorganic Chemistry*, University Science Books, Mill Valley, California, **1994**.
- [2] M. J. Romão, J. Knäblein, R. Huber, J. J. G. Moura, *Prog. Biophys. Molec. Biol.* **1997**, *68*, 121–144.
- [3] R. Calvo, E. C. Abresch, R. Bittl, G. Feher, W. Hofbauer, R. A. Isaacson, W. Lubitz, M. Y. Okamura, M. L. Paddock, *J. Am. Chem. Soc.* **2000**, *122*, 7327–7341.
- [4] A. Bencini, D. Gatteschi, *Electron Paramagnetic Resonance of Exchange Coupled Systems*, Springer, Berlin, **1989**.
- [5] S. K. Hoffmann, W. Hilczler, J. Goslar, *Appl. Magn. Reson.* **1994**, *7*, 289–321 and references therein.
- [6] M. C. G. Passeggi, R. Calvo, *J. Magn. Reson. A* **1995**, *114*, 1–11.

- [7] D. van der Helm, M. B. Lawson, E. L. Enwall, *Acta Crystallog. B* **1971**, *27*, 2411–2418.
- [8] C. C. Ou, D. A. Powers, J. A. Thich, T. R. Felthouse, D. N. Hendrickson, J. A. Potenza, H. J. Schugar, *Inorg. Chem.* **1978**, *17*, 34–40.
- [9] T. G. Fawcett, M. Ushay, J. P. Rose, R. A. Lalancette, J. A. Potenza, H. J. Schugar, *Inorg. Chem.* **1979**, *18*, 327–332.
- [10] A. Dijkstra, *Acta Crystallog.* **1966**, *20*, 588–590.
- [11] M. A. Hitchman, L. Kwan, L. M. Engelhardt, A. H. White, *J. Chem. Soc., Dalton Trans.* **1987**, 457–465.
- [12] P. R. Levstein, R. Calvo, E. E. Castellano, O. E. Piro, B. E. Rivero, *Inorg. Chem.* **1990**, *29*, 3918–3922.
- [13] R. Calvo, C. A. Steren, O. E. Piro, T. Rojo, F. J. Zuñiga, E. E. Castellano, *Inorg. Chem.* **1993**, *32*, 6016–6022.
- [14] R. F. Baggio, R. Calvo, C. D. Brondino, M. T. Garland, A. M. Atria, E. Spodine, *Acta Crystallog. C* **1995**, *51*, 382–385.
- [15] C. M. Gramaccioli, R. E. Marsh, *Acta Crystallog.* **1966**, *21*, 594–605.
- [16] L. Antolini, G. Marcotrigiano, L. Menabue, G. C. Pellacani, M. Saladini, M. Sola, *Inorg. Chem.* **1985**, *24*, 3621–3626.
- [17] F. S. Stephens, R. S. Vagg, P. A. Williams, *Acta Crystallog. B* **1974**, *27*, 841–845.
- [18] C. K. Johnson, ORTEP. Report ORNL-3794, Oak Ridge, TN, **1965**.
- [19] *International Tables for X-ray Crystallography*, Vol. IV, Kynoch Press, Birmingham, **1974**.
- [20] R. Calvo, M. A. Mesa, *Phys. Rev. B* **1983**, *28*, 1244–1248.
- [21] H. J. Zeiger, G. W. Pratt, *Magnetic Interactions in Solids*, Oxford University Press, London, **1973**.
- [22] A. M. Gennaro, P. R. Levstein, C. A. Steren, R. Calvo, *Chem. Phys.* **1987**, *111*, 431–438.
- [23] H. Yokoi, S. Ohsawa, *Bull. Chem. Soc. Japan* **1973**, *46*, 2766–2768.
- [24] P. R. Newman, J. M. Imes, J. A. Cowen, *Phys. Rev. B* **1976**, *13*, 4093–4097.
- [25] R. Calvo, H. Isern, M. A. Mesa, *Chem. Phys.* **1985**, *100*, 89–99.
- [26] P. M. Richards, M. B. Salamon, *Phys. Rev. B* **1974**, *9*, 32–45.
- [27] C. D. Brondino, N. M. C. Casado, M. C. G. Passeggi, R. Calvo, *Inorg. Chem.* **1993**, *32*, 2078–2084.
- [28] P. R. Levstein, C. A. Steren, A. M. Gennaro, R. Calvo, *Chem. Phys.* **1988**, *120*, 449–459.
- [29] A. M. Gennaro, R. Calvo, *J. Phys. Condens. Matter* **1989**, *1*, 7061–7068.
- [30] In Equations (3) and (4) a Heisenberg exchange Hamiltonian  $H_{ex} = -JS_i S_j$  was assumed.
- [31] EPR spectroscopy cannot determine the sign of the exchange interaction.
- [32] R. Calvo, M. C. G. Passeggi, M. A. Novak, O. G. Symko, S. B. Oseroff, O. R. Nascimento, M. C. Terrile, *Phys. Rev. B* **1991**, *43*, 1074–1083.
- [33] R. E. Rapp, H. Godfrin, R. Calvo, *J. Phys. Condens. Matter* **1995**, *7*, 9595–9606.
- [34] M. L. Siqueira, R. E. Rapp, R. Calvo, *Phys. Rev. B* **1993**, *48*, 3257–3263.
- [35] P. R. Levstein, R. Calvo, *Inorg. Chem.* **1990**, *29*, 1581–1582.
- [36] O. Kahn, *Molecular Magnetism*, VCH Publishers, Inc., New York, **1993**, chapter 8.
- [37] E. Colacio, M. Ghazi, R. Kivekäs, J. M. Moreno, *Inorg. Chem.* **2000**, *39*, 2882–2890 and references therein.
- [38] Z. Otwinowski, W. Minor in *Methods in Enzymology* (Eds.: C.W. Carter Jr., R. M. Sweet), Academic Press, New York, **1997**, *276*, 307–326.
- [39] G. M. Sheldrick, *SHELXS-97, Program for Structure Solution*, University of Göttingen, Göttingen, Germany, **1997**.
- [40] G. M. Sheldrick, *SHELXL-97, Program for Structure Refinement*, University of Göttingen, Göttingen, Germany, **1997**.

Received April 14, 2002  
[I02195]